Hot electron spin-valve effect in coupled magnetic layers

R. J. Celotta, J. Unguris, and D. T. Pierce
Electron Physics Group, National Institute of Standards and Technology, Gaithersburg, Maryland 20899

SEMPA observations of magnetic exchange coupling in the Fe/Ag/Fe, Fe/Au/Fe, and Fe/Cr/Fe systems reveal an intensity variation in the emitted secondary electron signal that depends only on whether the Fe layers are coupled in a ferromagnetic or antiferromagnetic sense. We ascribe this new effect to spin dependence in the transport of electrons between the two magnetic layers.

INTRODUCTION

The phenomena of exchange coupling of ferromagnetic layers and the related giant magnetoresistance effect (GMR) have been the subject of extensive recent research,[1] owing, in part, to the potential such effects have for application in a new class of devices called spin valves.[2] The GMR effect depends upon a difference in the spin-dependent transport of Fermi energy electrons between two or more ferromagnetic layers that are aligned either ferromagnetically or antiferromagnetically with each other. We have discovered a similar effect, an alignment-dependent variation in the emission of secondary electrons, in Fe/Ag/Fe, Fe/Au/Fe, and Fe/Cr/Fe sandwiches. We ascribe this new effect to spin-dependent transport of much higher energy electrons, i.e., hot electrons with energies of 5–15 eV with respect to the Fermi level.

In a series of measurements, we have applied the technique of scanning electron microscopy with polarization analysis[3] (SEMPA) to the study of the Fe/Cr/Fe,[4] Fe/Ag/Fe,[5] and Fe/Au/Fe[6] exchange coupled layers. The experimental arrangement we have used for our SEMPA studies of exchange coupling in Fe/Ag/Fe is shown in Fig. 1. Although we have obtained similar results for the Fe/Cr/Fe and Fe/Au/Fe systems, we will illustrate this new effect in this paper by concentrating on measurements of the Fe/Ag/Fe system.

An Fe single crystal whisker is used for the substrate because of its very high degree of crystalline perfection and surface flatness. A Ag film is grown epitaxially in the shape of a wedge with its thickness varying from 0 to 25 ML. Finally, an Fe overlayer is grown with a uniform thickness in the range of 3–12 ML. The domain structure of the Fe substrate is very simple; it consists of two oppositely oriented domains, as shown in Fig. 1. As a result of the periodic reversal of exchange coupling as a function of interlayer thickness, domains in the Fe overlayer will be oriented either parallel or antiparallel to the substrate domains depending on the sign of the coupling, and will form a pattern that directly reflects the periodicity of the coupling. The SEMPA instrument[3] can directly observe this magnetization pattern by measuring the polarization of the secondary electrons produced by the incident beam of a scanning electron microscope. In this way, very accurate determinations of the periods of the exchange coupling can be made and used to test the prevailing theory, in which the oscillations are correlated with the existence of nesting vectors in the Fermi surface of the interlayer material.[7,8]

In general, in SEMPA measurements the magnetization information is carried by the polarization of the secondary electrons, and is not reflected in the secondary electron intensity. However, measurements of sandwich structures with Fe whisker substrates, Fe overlayers, and Ag, Cr, and Au interlayers, reveal a very interesting secondary intensity signal, which *depends only on the relative alignment of the substrate and overlayer magnetization.* We attribute this signal to the propagation of energetic, or "hot," electrons from the substrate experiencing spin-dependent interactions during transport. Following a discussion of the specifics of the experimental procedure and results, we discuss our model for this effect.

EXPERIMENT

Complete details of the experimental procedure exist elsewhere.[3,4] The Fe(100) single crystal whiskers were cleaned with standard procedures,[9] and examined using SEMPA, reflection high energy electron diffraction (RHEED); and scanning Auger microscopy. Under inspection by scanning tunneling microscopy,[10] these Fe whisker surfaces are seen to be extremely flat with single atom high steps approximately every 1 μm. RHEED patterns of the Fe whiskers show a Laue arc of sharp spots after the whiskers are cleaned by Ar sputtering and annealed at 800 °C.

The interlayer wedge is grown by evaporating Ag at a rate between 0.07 and 0.8 monolayers/s while moving a shutter over the surface of the whisker. Growth at substrate temperatures between 60 °C and 100 °C produced RHEED patterns indicative of nearly perfect layer-by-layer growth. The observation of RHEED intensity oscillations indicated somewhat disordered growth for the first 3–4 layers, with much better growth for Ag thicknesses of 6–30 layers, followed by increasing disorder.

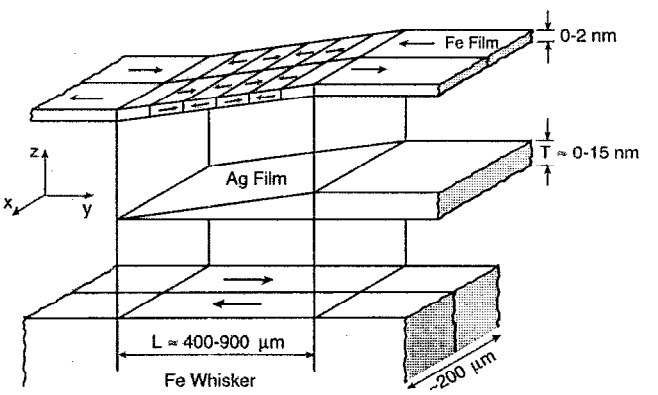

FIG. 1. Schematic diagram of Fe/Ag/Fe sandwich nanostructure showing the modulation in the sign of exchange coupling between Fe films.

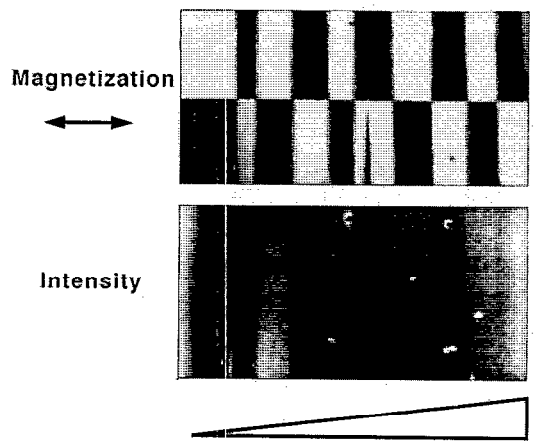

FIG. 2. Top: Magnetization image of wedge area. White (black) indicates magnetization to the right (left). Bottom: Intensity image of same region. Linear gray scale mapping with white indicating high intensity.

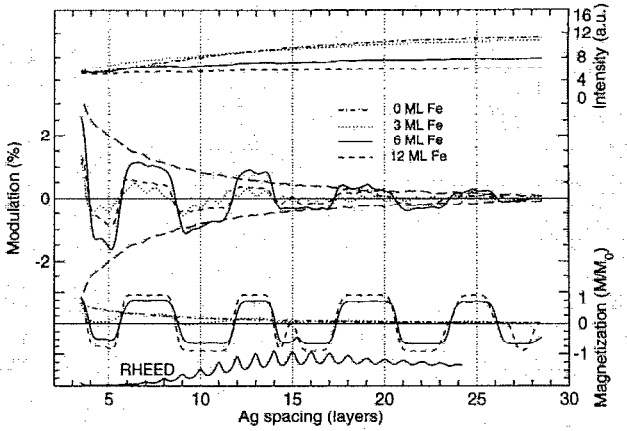

FIG. 3. Top: secondary intensity; center: modulation of secondary intensity; polarization envelope of 0 ML Fe secondaries (long dashes; see the text); bottom: normalized magnetization; RHEED intensity oscillations.

SEMPA images from the measurement of an Fe/Ag/Fe sandwich structure are shown in Fig. 2. The top image is the conventional SEMPA magnetization image, while the bottom image is the related secondary electron intensity image with its zero suppressed to better display the band-like intensity variations. Notice that while the two domain substrate structure creates a checkerboard pattern in the magnetization image, only bands are seen in the intensity. The secondary intensity image data can be reduced to a series of curves by computing, at each position along the wedge, i.e., each interlayer thickness, the secondary intensity averaged over the width of the wedge. The SEMPA magnetization image data is similarly reduced to curves, except the averaging is done within each of the two substrate domains and symmetry is invoked to correct for any instrumental zero offset in the magnetization measurement. The thickness scale can be determined very accurately by a method similar to the conventional method of monitoring RHEED intensity oscillations during evaporation. Instead, the microscope's electron beam is used to generate a RHEED image from a spot on the wedge portion of the sample. The intensity of a selected region of this image is used to form a "RHEED intensity image" as the incident beam scans the sample. The RHEED intensity image exhibits oscillations in intensity with the increasing thickness of the wedge. When correlated with the measured magnetization images by defect matching, the RHEED intensity image allows setting the thickness scale at every point of the magnetization or SEM intensity images to within ± 0.1 layers. The data are summarized in Fig. 3, where the lower curve shows the measured RHEED intensity oscillations for the first 20 layers of a wedge.

The topmost curves of Fig. 3 present the secondary electron intensity for Fe overlayer thicknesses of 3, 6, and 12 monolayers. Most notable is the rise in intensity in the 3 ML Fe curve as a function of Ag wedge thickness. This is presumably due to a greater secondary yield for Ag relative to Fe. When the background is subtracted from these curves by estimating it with a smoothly varying, low-order polynomial, a very interesting structure is revealed. These curves are replotted with their smoothly varying background subtracted in the middle of Fig. 3. The obvious modulation is presented as a percentage of the average intensity value at each Ag thickness. This modulation is seen for 3, 6, and 12 ML Fe overlayers, and closely mirrors the measured oscillation in the Fe/Ag/Fe interlayer exchange coupling. The amplitude of the modulation is greatest for a 6 ML Fe coverage, and the modulation amplitude is seen to decrease for all Fe thicknesses as the Ag thickness increases.

Below the intensity curves just discussed, we plot the magnetization measured in the positive y direction along the whisker. All magnetization values are shown normalized to the observed magnetization of bulk Fe, M_0. There are four curves here corresponding to Fe overlayer thicknesses of 0, 3, 6, and 12 ML. The 0 ML curve reflects the polarization of the Fe substrate as a function of Ag thickness, and we see an exponential falloff as the substrate polarization is attenuated by the increasing Ag interlayer thickness. The other magnetization curves display the expected[5,7] modulation of overlayer magnetization from exchange coupling. We note that it is not until an overlayer thickness of 12 ML that the full, bulk Fe magnetization is realized.

The correspondence between the modulation in the magnetization curves, with Ag thickness, and the modulation in the intensity curves, is obvious and striking. One might be led to the conclusion that the direction of magnetization of the Fe overlayer somehow affects the number of secondary electrons ejected. However, the Fe whisker substrate has two oppositely directed domains, as shown in Fig. 1, so the Fe overlayer domain structure is split into two halves with two oppositely directed magnetizations at each Ag thickness, also as shown in Fig. 1. If the overlayer magnetization from the other half of the Fe whisker were plotted, the curves would look as if they had been inverted with respect to the x axis. The intensity curves from this half of the whisker do not invert, however. Hence, *the intensity oscillations are correlated with the relative alignment of magnetization of the Fe films.*

DISCUSSION

The electrons used to form images in the SEMPA technique are secondary electrons. They are generated from the

cascade of incident primary electrons or backscattered electrons, and originate from a region within a few nanometers of the surface because of mean-free path considerations. The electrons that contribute to the signals displayed in Fig. 3 may originate in the Fe substrate, the Ag interlayer, or the Fe overlayer, depending on the particular situation. For example, the 0 ML Fe magnetization curve is seen to exhibit an approximately exponential decay with Ag thickness. This decrease in polarization corresponds to the increased number of unpolarized electrons originating in the Ag accompanied by the attenuation of the polarized secondary electrons from the Fe substrate. This 0 ML polarization curve has been scaled and replotted, with its mirror image, in the middle of Fig. 3. The envelope created suggests that the falloff in intensity modulation amplitude with Ag thickness is related to the relative abundance of secondary electrons from the substrate.

The explanation of the observed effect lies in the filtering of hot electrons due to spin-dependent scattering, and is directly analogous to explanations of the basis for the giant magnetoresistance in similar sandwich structures. Incident primary electrons, and other electrons in the cascade, generate polarized electrons in the substrate, some of which are directed toward the surface. These electrons are attenuated during their transport to the surface by spin-dependent as well as spin-independent interactions. Transport through the Ag interlayer may be presumed to occur in a spin-independent manner. However, there may be spin-dependent interactions within the Fe overlayer or at the Ag/Fe interface. For example, there have been both theoretical[11,12] and experimental[13,14] determinations of spin-dependent mean-free paths in bulk materials, as well as a discussion[15] of using the difference in mean-free path as the basis of a spin detector. The spin-dependent interactions, which depend only on the relative alignment of the magnetic layers, control the number of substrate electrons that make it to the near surface region. However, since the measured electron polarization is constant for all but the smallest Ag interlayer thicknesses, the secondary electrons ejected reflect the overlayer polarization and must originate there. The experimental results can therefore be explained by spin-dependent, hot electron transport of substrate electrons to the near surface region, followed by the ejection of polarized overlayer electrons with an intensity modulation that reflects the spin dependence of the transport.

The secondary electrons from the substrate, which must have an energy nominally greater than 5 eV above the Fermi level, experience a few percent difference in transmission probability for the two cases of parallel and antiparallel ferromagnetic layer alignment. As in the GMR effect, the transport is higher for the parallel magnetization configuration. However, the GMR phenomena is related to Fermi level electrons, while those playing a role here are obviously of a much higher energy.

We have made similar measurements in the Fe/Au/Fe and Fe/Cr/Fe systems, as shown for comparison, along with the Fe/Ag/Fe data in Fig. 4. In both cases the measured secondary intensity is modulated and the modulation correlates directly with the relative alignment between the ferromagnetic layers. As was the case in Ag, aligned ferromagnetic layers produce higher secondary electron intensities.

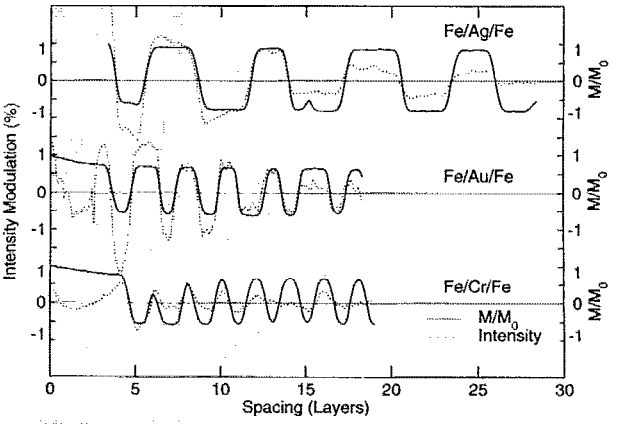

FIG. 4. Relationship between secondary intensity oscillations (dotted lines, scales to left) and magnetization direction (solid lines, scales to right).

CONCLUSION

We report a modulation in the production of near surface secondary electrons in Fe sandwich structures that depends on the relative orientation of the two Fe layers, when separated by Ag, Au, or Cr. The modulation in amplitude, of a few percent, is seen to be due to the spin-dependent transport of hot electrons between the Fe substrate and the Fe overlayer, resulting in the ejection of an overlayer electron. Parallel alignment of the Fe layers, in the cases we studied, always corresponds to a higher secondary emission current.

ACKNOWLEDGMENTS

We wish to acknowledge the support of the Technology Administration of the U.S. Department of Commerce and the Office of Naval Research. The Fe whiskers were grown at Simon Fraser University under an operating grant from the National Science and Engineering Research Council of Canada.

[1] See, for example, *Ultrathin Magnetic Structures*, edited by B. Heinrich and J. A. C. Bland (Springer, New York, 1993).
[2] B. Dieny , V. S. Speriosu, S. S. P. Parkin, B. A. Gurney, D. R. Wilhoit, and D. Mauri, Phys. Rev. B **43**, 1297 (1991).
[3] M. R. Scheinfein, J. Unguris, M. H. Kelley, D. T. Pierce, and R. J. Celotta, Rev. Sci. Instrum. **61**, 2501 (1990).
[4] J. Unguris, R. J. Celotta, and D. T. Pierce, Phys. Rev. Lett. **67**, 140–143 (1991).
[5] J. Unguris, R. J. Celotta, and D. T. Pierce, J. Magn. Magn. Mat. **127**, 205 (1993).
[6] J. Unguris, R. J. Celotta and D. T. Pierce, J. Appl. Phys. (these proceedings).
[7] M. D. Stiles, Phys. Rev. B **48**, 7238 (1993).
[8] K. B. Hathaway, and references therein, in Ref. 1.
[9] S. T. Purcell, A. S. Arrott, and B. Heinrich, J. Vac. Sci. Technol. B **6**, 794 (1988).
[10] J. A. Stroscio, D. T. Pierce, and R. A. Dragoset, Phys. Rev. Lett. **70**, 3615 (1993); J. A. Stroscio and D. T. Pierce, Proceedings of STM'93, Beijing, China, J. Vac. Sci. Technol. (in press).
[11] D. R. Penn, S. P. Apell, and S. M. Girvin, Phys. Rev. Lett. **55**, 518 (1985); Phys. Rev. B **32**, 7753 (1985).
[12] J. Glazer and E. Tosatti, Solid State Commun. **52**, 905 (1984).
[13] D. P. Pappas, K.-P. Kämper, B. P. Miller, H. Hopster, D. E. Fowler, C. R. Brundle, A. C. Lunty, and Z.-X. Shen, Phys. Rev. Lett. **66**, 504 (1991).
[14] H. Hopster, and references therein, in Ref. 1.
[15] G. Schönhense and H. C. Siegmann, Ann. Phys. **2**, 465 (1993).